The Influence of Microwave Magnetic Field Gradient on ODMR Line Width

Zihan Li[1,a,*], Shaohui Meng[1,b], Senhao Zhao[1,c], Shuo Lin[1,d], Jianqiang Lu[1,e], Zihao Wang[1,f]

[1]School of Communication and Information Engineering, Nanjing University of Posts and Telecommunications, Xiaolingwei Street, Nanjing, China

[a]b22011016@njupt.edu.cn, [b]b22010425@njupt.edu.cn, [c]b22010525@njupt.edu.cn, [d]b22011522@njupt.edu.cn, [e]b22011727@njupt.edu.cn, [f]b22012507@njupt.edu.cn

*Corresponding author

Keywords: nitrogen-vacancy (nv) centers, optically detected magnetic resonance (odmr), quantum computing, magnetic field gradient, spectral line width, lorentzian profile

Abstract: The development of modern quantum technologies, such as quantum computing and quantum communication, relies on the use of qubits, a novel computational method distinct from classical bits. The nitrogen-vacancy (NV) center, with its excellent optical properties and strong coherence, has been highly praised by both the physics and engineering communities as an outstanding qubit. It is widely applied in experiments such as quantum key distribution and biological fluorescence labeling. The spin of the NV center can be manipulated and detected using lasers and microwaves. Additionally, due to its electron spin coherence time reaching the millisecond level, the NV center is considered a highly promising system for quantum computing. Experiments utilizing NV quantum registers and quantum error correction have been demonstrated. Moreover, NV centers can also serve as nanoscale sensors for measuring physical quantities such as magnetic fields, electric fields, and temperature. Internationally, NV centers have been used to detect nuclear magnetic resonance signals in organic materials and to measure temperature within biological cells. Another technology with comparable impact to the NV center is Optically Detected Magnetic Resonance (ODMR), which generates spectral lines through the double resonance phenomenon between the intrinsic vibrations of molecules or atoms and externally applied microwaves. Obtaining high-quality spectral lines, i.e., those closely matching the ideal model, is of crucial importance for both scientific research and industrial production. In this paper, we first introduce the physical basis of the NV center, including its physical structure, energy level structure, and the eight-peak curve of optically detected magnetic resonance. We then analyze the line shape of the ODMR spectrum and demonstrate that it follows a Lorentzian profile. Finally, we prove the effect of magnetic field gradient on the spectral line width (full width at half maximum, FWHM).

1. Introduction

In recent years, the rapid development of quantum technology, exemplified by quantum computing and quantum communication, has sparked the wave of a second industrial revolution in information technology. Unlike classical computers that operate with classical bits, quantum computers introduce the concept of quantum bits (qubits) [1]. In classical computing, the basic unit of computation is the classical bit, which can take the values 0 or 1, corresponding to low and high voltage levels, respectively. A sequence of 0s and 1s arranged in a specific order forms a bit string that corresponds to a particular electrical pulse signal, which is transmitted via antennas for communication. The fundamental unit of classical communication is the classical bit, and due to the limitations of its binary nature, the computational power of classical computers has reached its limits, failing to meet the diverse needs of modern information technology [2].

1.1. Nitrogen-Vacancy (NV) Centers in Diamond

Quantum computing, by enriching the values of computational units, has broken through the limitations imposed by the binary nature of classical bits and innovatively introduced the concept of

  DOI: 10.25236/icmmct.2025.008

the “quantum bit” or “qubit” [3]. In the concept of quantum bits, the two classical values of 0 and 1 are regarded as two quantum states $|0\rangle$ and $|1\rangle$. By leveraging the superposition principle in quantum mechanics, a qubit is constructed as $|\psi\rangle = \alpha|0\rangle + \beta|1\rangle$, where α and β are complex coefficients. This qubit can be represented on the Bloch sphere.

This approach thus enriches the possible values of a quantum bit. Traditional bits are represented by the voltage levels 0 and V on a capacitor, whereas quantum bits are represented by a two-level energy system. If a series of quantum bits can be stored, it is possible to emulate the encoding mode of classical bits to achieve the encoding of quantum states.

With the deepening of research, a variety of particles suitable for use as quantum bits have emerged rapidly, like bamboo shoots after a spring rain: photons, electrons, ion traps, and so on. Among them, the nitrogen-vacancy (NV) center in diamond has stood out due to its unique optical properties, winning the favor of physicists and finding widespread application in fields such as electronics, radio communications, and quantum communications [4, 5].

1.2. The Physical Structure of Nitrogen-Vacancy (NV) Centers

In the diamond crystal lattice, locations where the structural integrity is disrupted are referred to as crystal defects. Among these defects, point defects that selectively absorb light in the visible spectrum are known as “color centers.” To date, scientists have identified over 500 distinct types of color centers. The nitrogen-vacancy (NV) center in diamond refers to a stable configuration formed when a nitrogen atom (Nitrogen, N) replaces a carbon atom (Carbon, C) in the diamond lattice, and an adjacent carbon atom is missing, creating a vacancy [6]. This specific arrangement of the nitrogen atom and the vacancy is depicted in Figure 1.

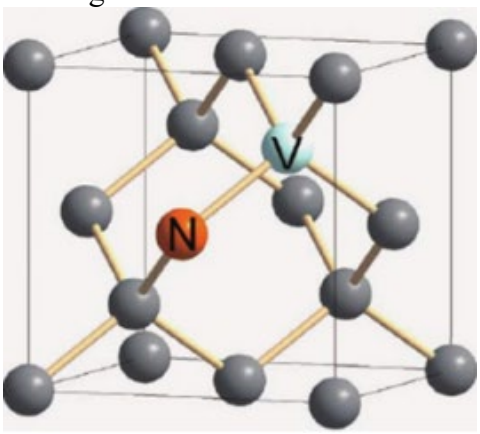

Figure 1 This caption has one line so it is centred.

The nitrogen-vacancy (NV) center is a type of defect in diamond, consisting of a nitrogen atom (N) that substitutes for a carbon atom (C) and an adjacent lattice vacancy, as shown in Figure 1. There are two primary forms of NV centers: NV0 and NV−. The negatively charged NV− center is the focus of quantum technological applications. It contains six electrons in its structure: two from the nitrogen atom, three from the carbon atoms adjacent to the vacancy, and one from a captured donor impurity. The NV− center exhibits C3V symmetry. The axis of the NV center is defined by the line connecting the nitrogen and vacancy sites, and there are four distinct orientations of this axis in the diamond lattice, with each pair of axes forming an angle of 109.5°.

1.3. Energy Level Structure of NV Color Centers and Optical Detection of Magnetic Resonance

The research indicates that the NV color center consists of four orbitals, all of which are occupied by single electrons. Moreover, the energy levels of these orbitals increase progressively. Therefore, the electronic structure of the NV color center can be understood as the matching of six electrons with four orbitals. This experimental model has been validated by electron paramagnetic resonance (EPR) and supported by first-principles calculations of the NV- center, as well as theoretical studies [7].

The energy levels of the NV color center include the ground-state spin triplet ($3A_2$), the excited-state spin triplet (3E), and two special metastable states ($1A_1$ and 1E). Among them, the ground-state

$3A_2$ and the excited-state 3E both have spin quantum levels of ms = 0 and ms = ±1, which together form two quantum two-level structures as shown in Figure 2.

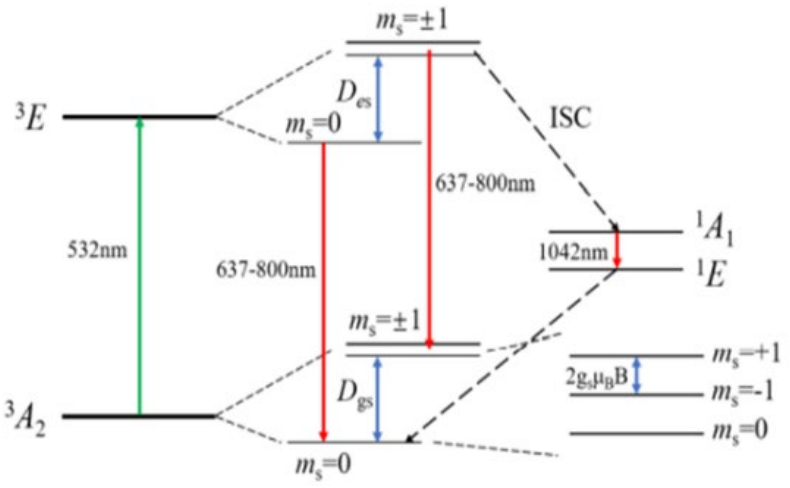

Figure 2 Energy Level States of NV Color Centers

The ground-state $3A_2$ of the NV color center has degenerate ms = ±1 states, which are split from the ms = 0 state by a zero-field splitting with a splitting strength of Dgs = 2.87 GHz. However, when an external static magnetic field B is applied along the NV axis, the degeneracy of the ms = ±1 states is lifted through the Zeeman effect, resulting in two sub-levels: ms = +1 and ms = −1. Specifically, the ms = +1 state shifts to a higher energy level, while the ms = −1 state shifts to a lower energy level. The degree of splitting is directly proportional to the magnitude of the external static magnetic field B.

Under the influence of an external axial static magnetic field B [8], the Hamiltonian of the ground state of the nitrogen-vacancy (NV) color center can be expressed as:

$$H = H_s + H_{sl} + H_l \tag{1}$$

The three components can be further written as:

$$\begin{cases} H_s = D_{gs}S_z^2 + E\left(S_x^2 - S_y^2\right) + g_s\mu_B\vec{B}\cdot\vec{S} \\ H_{sl} = A_{\parallel}S_zI_z + A_{\perp}\left(S_xI_x + S_yI_y\right) \\ H_l = PI_z^2 - g_I\mu_N\vec{B}\cdot\vec{S} \end{cases} \tag{2}$$

In the equation, $S = \{S_x, S_y, S_z\}$ represents the spin matrices of the electron.

The unique spin triplet states of the NV color center can be described by a set of wave functions. The evolution of these wave functions follows the Schrödinger equation. By solving the eigenvalues and eigenvectors of the Hamiltonian, the wave functions and energy levels of each state can be obtained. The distribution of a large number of NV color centers among the various energy levels follows the Boltzmann distribution.

In a single nitrogen-vacancy (NV) color center in diamond, there are only six possible energy level transition pathways. However, for multiple NV color centers within a bulk diamond crystal, there are a total of 24 possible transition pathways. This is because the multiple NV color centers in the bulk diamond crystal exist in four different orientations. As a result, the projection strength of the external static magnetic field along the four different NV axes is also different. When a resonant microwave signal is applied, NV color centers with different orientations correspond to different resonant microwave frequencies. Specifically, for one NV axis orientation, there are two distinct resonant frequencies: one for the transition from the ground-state ms = 0 level to the ms = +1 level, and the other for the transition to the ms = −1 level. Therefore, the four NV axis orientations collectively have eight different resonant microwave frequencies, which manifest as eight main resonant peaks in the optically detected magnetic resonance (ODMR) spectrum. Additionally, due to the hyperfine

structure in the NV color centers, each main resonant absorption peak contains three sub-peaks, resulting in a total of 24 resonant absorption peaks corresponding to the 24 transition pathways.

Considering the combined effects of the intrinsic quantum noise of the diamond NV color centers and the applied microwave magnetic field, the resonant absorption peaks are broadened. Therefore, in practice, the small resonant peaks are often not observed in the ODMR spectrum, and only the eight main peaks are visible, as shown in Figure 3.

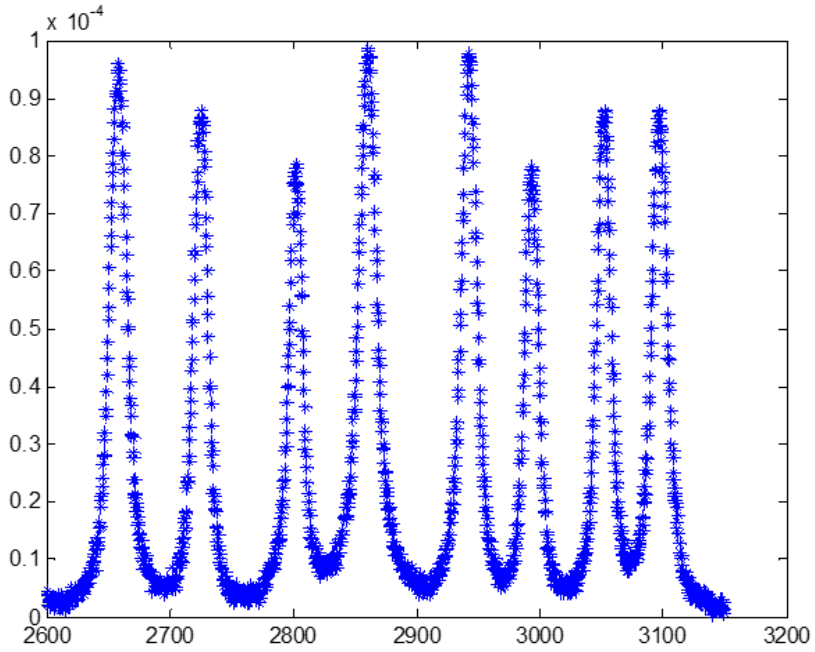

Figure 3 Energy Level States of NV Color Centers

2. Optically Detected Magnetic Resonance (ODMR) Curve

In 1950, the French physicist Kastler pioneered the experimental method of optically detected magnetic resonance (ODMR) [9]. Optically Detected Magnetic Resonance (ODMR) refers to the phenomenon of simultaneous occurrence of optical-frequency resonance in atoms or molecules and magnetic resonance at radio-frequency or microwave frequencies, known as double resonance.

The fundamental idea behind ODMR is to use the pumping effect of light to create a polarization of the population distribution among the Zeeman sublevels of the atomic ground state. Then, by employing magnetic resonance, this polarized population distribution is perturbed, leading to a change in the pumping rate of the light. By detecting these changes in the pumping rate, the structure of the atomic Zeeman levels can be studied.

ODMR technology ingeniously combines the high sensitivity of optical detection with the high resolution of magnetic resonance [10], integrating both optical and magnetic resonance techniques. It is a prime example in terms of experimental design. This technique can be used to study the fine and hyperfine structures of atoms or molecules and has the potential for quantum precision measurements. Due to its significant applications in fundamental physical research and the measurement of weak magnetic fields, Kastler was awarded the Nobel Prize in 1966.

2.1. Rabi Oscillations

For a two-level system, when an electromagnetic wave is applied at an appropriate frequency, the atoms in the system will continuously undergo transitions between the energy levels E1 and E2. This phenomenon is known as Rabi oscillations. The oscillation process is a stochastic process. We study a particle undergoing Rabi oscillations using statistical methods and find that the probability of a particle in the ground state being excited to the excited state follows a sinusoidal squared distribution. Moreover, when the frequency of the applied light field is far from the resonance line of the two

energy levels, the interaction between the field and the atom is lost.

The evolution of the wave function of a particle undergoing Rabi oscillations satisfies unitary evolution.

$$\begin{aligned} |\psi(t)\rangle &= U_{old}(t)|\psi(0)\rangle \\ &= \begin{pmatrix} \cos\frac{\Omega t}{2} & -i\sin\frac{\Omega t}{2} \\ -i\sin\frac{\Omega t}{2} & \cos\frac{\Omega t}{2} \end{pmatrix}\begin{pmatrix} 0 \\ 1 \end{pmatrix} \\ &= \cos\frac{\Omega t}{2}|g\rangle - i\sin\frac{\Omega t}{2}|e\rangle \end{aligned} \tag{3}$$

Where $\{|e>, |g>\} = \frac{1}{2}\begin{pmatrix} 0 & \Omega \\ \Omega & 0 \end{pmatrix}$. The first term in the equation represents the ground state, while the second term represents the excited state, indicating that the probabilities of being in the ground state and the excited state are respectively:

$$P_g(t) = \cos^2\frac{\Omega t}{2} \tag{4}$$

$$P_e(t) = \sin^2\frac{\Omega t}{2} \tag{5}$$

2.2. Derivation of ODMR Line Width

We know that the NV color center is a spin triplet, and it becomes spin-polarized under optical excitation. Meanwhile, the degenerate states undergo Zeeman splitting in the presence of a magnetic field, resulting in eight peaks. To investigate the spectral line shapes of these peaks, we first employ perturbation theory to study the Schrödinger equation of a two-level system.

$$\widehat{H} = \widehat{H}_0 + \widehat{H}_1(t) \tag{6}$$

$$\widehat{H}\Psi = E\Psi \tag{7}$$

Where, $\widehat{H}_1(t)$ is the perturbation term, originating from the optical field.

Let the stationary states corresponding to the two energy levels of the two-level system be φ_1 and φ_2, representing the ground state and the excited state, respectively. These stationary states are determined by the time-independent Schrödinger equation, so:

$$\widehat{H}_0\varphi_1 = E_1\varphi_1 \tag{8}$$

$$\widehat{H}_0\varphi_2 = E_2\varphi_2 \tag{9}$$

Correspondingly, by multiplying the time factor, we obtain the wave functions:

$$\Psi_1(\vec{\gamma}, t) = \varphi_1(\vec{\gamma})e^{-i\omega_1 t} \tag{10}$$

$$\Psi_2(\vec{\gamma}, t) = \varphi_2(\vec{\gamma})e^{-i\omega_2 t} \tag{11}$$

According to the principle of superposition of states, we have:

$$\Psi(\vec{\gamma}, t) = C_1(t)\varphi_1(\vec{\gamma})e^{-i\omega_1 t} + C_2(t)\varphi_2(\vec{\gamma})e^{-i\omega_2 t} \tag{12}$$

The coefficients should satisfy the normalization condition:

$$|C_1(t)|^2 + |C_2(t)|^2 = 1 \tag{13}$$

Time-dependent Schrödinger equation:

$$\mathrm{i}\hbar\frac{\partial}{\partial \mathrm{t}}\Psi = \widehat{\mathrm{H}}\Psi \tag{14}$$

Then, we obtain:

$$\mathrm{i}\dot{\mathrm{C}}_1 = \Omega\cos(\mathrm{cot})e^{-i\omega_0 t}\,\mathrm{C}_2 \tag{15}$$

$$\mathrm{i}\dot{\mathrm{C}}_2 = \Omega\cos(\mathrm{cot})e^{-i\omega_0 t}\,\mathrm{C}_2 \tag{16}$$

where $\omega_0 = \frac{E_2 - E_1}{\hbar}$, Ω is the frequency of the Rabi oscillation:

$$\Omega = \frac{e}{\hbar} \int \varphi_1^*(\gamma) \vec{\gamma} \vec{E}_0 \varphi_2(\gamma) d^3\vec{\gamma} \tag{17}$$

Here, $\vec{\gamma}$,$\vec{E}_0$ represent the amplitude of the applied light field, while E represents the electric field strength. If the initial state is such that all atoms are in the state φ_1, which corresponds to the lower energy level, then:

$$C_1(0) = 1 \tag{18}$$

$$C_2(0) = 0 \tag{19}$$

Then, we obtain:

$$C_1(t) = 1 \tag{20}$$

$$C_2(t) = \frac{\Omega}{2} \left\{ \frac{1 - exp[i(\omega_0 + \omega)t]}{\omega_0 + \omega} + \frac{1 - exp[i(\omega_0 - \omega)t]}{\omega_0 - \omega} \right\} \tag{21}$$

Therefore, based on the physical meaning of $C_2(t)$, the square of its modulus represents the probability of the particle transitioning to the second energy level:

$$|C_2(t)|^2 = \left| \Omega \frac{\sin(\omega_0 - \omega)t/2}{\omega_0 - \omega} \right|^2 \tag{22}$$

Since the perturbation of the atomic system by the microwave field is very weak, we should assume that $\omega_0 + \omega$ and $\omega_0 - \omega$ are very small. Therefore, Equation (16) can be written as:

$$i\dot{C}_1 = C_2 \left[e^{i(\omega_0 - \omega)t} + e^{-i(\omega_0 + \omega)t} \right] \frac{\Omega}{2} \tag{23}$$

Compared to $e^{i(\omega_0 - \omega)t}, e^{-i(\omega_0 + \omega)t}$ oscillates much more rapidly, so we can make the approximation:

$$i\dot{C}_1 = C_2 e^{i(\omega_0 - \omega)t} \frac{\Omega}{2} \tag{24}$$

$$i\dot{C}_2 = C_1 e^{i(\omega_0 + \omega)t} \frac{\Omega}{2} \tag{25}$$

It can be combined and written as:

$$\ddot{C}_2 + i(\omega_0 - \omega)\dot{C}_2 + \left| \frac{\Omega}{2} \right|^2 C_2 = 0 \tag{26}$$

Given the initial conditions $C_1(0) = 1, C_2(0) = 0$, we can solve for:

$$|C_2(t)|^2 = \frac{\Omega^2}{W^2} \left[\sin\left(\frac{\omega t}{2} \right) \right]^2 \tag{27}$$

Where:

$$W^2 = \Omega^2 + (\omega_0 - \omega)^2 \tag{28}$$

In the experiment, by controlling the duration of the microwave interaction such that the sine factor reaches its maximum value, the fluorescence intensity of the ODMR spectral line is proportional to $\frac{\Omega^2}{W^2}$, where $\omega_0 - \omega$ is the detuning. It can be observed that the spectral line follows a Lorentzian distribution, with the peak of the microwave frequency corresponding exactly to the resonance absorption peak of the two-level system.

3. The Impact of Magnetic Field Gradient on ODMR Line Width

3.1. Theoretical Derivation

In quantum mechanics, energy can be represented as the eigenvalue of the Hamiltonian operator. The Hamiltonian operator for an electron can be expressed by the following equation:

$$\widehat{H} = \mu_B \vec{B} \cdot \vec{g}\hat{s} \tag{29}$$

Here, B represents the magnetic field strength, $\vec{g}$ is the gyromagnetic factor matrix, and $\hat{s}$ is the spin matrix. The term $\vec{B} \cdot \vec{g}\hat{s}$ describes the interaction between the magnetic field and the electron spin.

$$\hat{s} = \frac{\hbar}{2}\left(\hat{\sigma}_x, \hat{\sigma}_y, \hat{\sigma}_z\right) \tag{30}$$

Therefore, H is a matrix. Since the electron spin is1/2, there are two possible values for the spin projection: ms=±1/2. For the NV center's spin triplet state, there are three observed spin states: ms=0 and ms=±1. The energy difference between the eigenvalues corresponding to the ms=±1 states represents the energy difference related to the ODMR line width. In the ODMR spectrum, each fluorescence contrast on the absorption peak (except for the peak itself) corresponds to two frequencies of the applied microwave field. These two frequencies correspond to the energy of the NV center ms=±1 states absorbing or emitting a photon, matching the energy difference involved in the transition, thus producing the ODMR spectrum. Therefore, the energy associated with the ms=±1 states (i.e., the difference in the eigenvalues of the Hamiltonian matrix) reflects the ODMR line width. We can represent H as a matrix:

$$\widehat{H} = \frac{1}{2}\hbar\mu_B g \cdot \begin{bmatrix} B_z & \frac{1}{\sqrt{2}}\left(B_x - iB_y\right) & 0 \\ \frac{1}{\sqrt{2}}\left(B_x + iB_y\right) & 0 & \frac{1}{\sqrt{2}}\left(B_x - iB_y\right) \\ 0 & \frac{1}{\sqrt{2}}\left(B_x + iB_y\right) & -B_z \end{bmatrix} \tag{31}$$

We have three eigenvalues:

$$E_+ = \frac{1}{2}\hbar\mu_B gB \quad E_- = -\frac{1}{2}\hbar\mu gB \quad E_0 = 0 \tag{32}$$

Additionally, the energy difference between the ms=±1 states is:

$$\mathrm{B} = \sqrt{\mathrm{B}_\mathrm{x}^2 + \mathrm{B}_\mathrm{y}^2 + \mathrm{B}_\mathrm{z}^2} \tag{33}$$

$$\Delta E = E_+ - E_- = \hbar\mu_B gB \tag{34}$$

The frequency difference is given by:

$$\Delta\omega = \frac{\Delta E}{\hbar} = \mu_B gB \tag{35}$$

To study a magnetic field with a gradient, we can expand it based on the gradient and retain the first-order terms:

$$\Delta\omega\left(\vec{r}\right) = \Delta\omega_0 + \sum_i \left.\frac{\partial\Delta\omega}{\partial r_i}\right|_{\vec{r_0}} \left(\mathrm{r_i} - \mathrm{r_{0_i}}\right) \tag{36}$$

Here, ω_0 represents the reference ODMR frequency, which is the value at the center of the antenna. The equation can be written as:

$$\Delta\omega\vec{\mathrm{r}} = \overrightarrow{\mathrm{r_0}} \tag{37}$$

$$\Delta\omega = \Delta w_0 + \mu_B g|\nabla B| \tag{38}$$

Here, ∇B represents the gradient of the magnetic field. It can be seen that the linewidth of the ODMR spectrum increases with the increase of the magnetic field gradient. For a perfectly uniform magnetic field, the spectral line is the narrowest. Ideally, the spectral line should be an infinitely narrow line. However, in reality, even when the external magnetic field is completely uniform and zero, the spectral line still has a certain width. This originates from the inherent effects of the atomic nuclei themselves, such as spin and relaxation processes. The presence of a magnetic field gradient can cause microwave interactions with the intrinsic magnetic moments of the atomic nuclei, reducing

the resonance absorption intensity. Therefore, theoretically, where the magnetic field gradient is small, the spectral line is tall and narrow; conversely, where the magnetic field gradient is large, the spectral line is short and broad.

3.2. Experimental Validation

We conducted experiments using antenna samples. The magnetic field distribution in the antenna is shown in Figure 4.

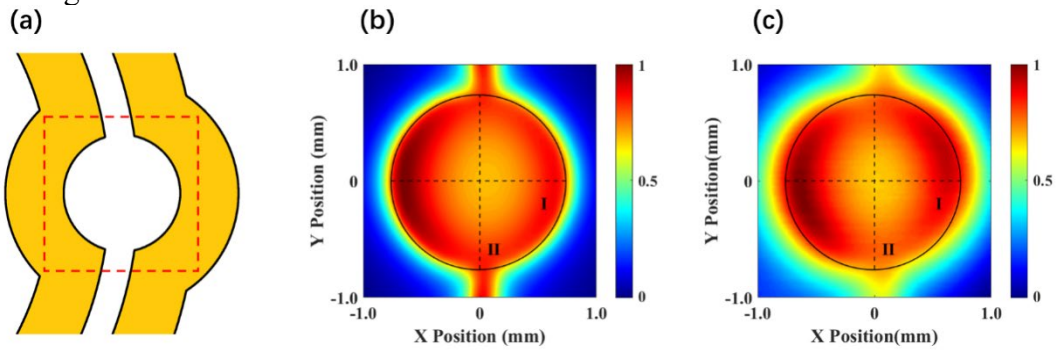

Figure 4 Magnetic Field Distribution in the Antenna

It can be observed that the magnetic field gradient increases as the position gets closer to the center. The ODMR spectra obtained from experiments conducted at the center and the edge are shown in Figures 5 and Figure 6, respectively. It can be seen that the experimental results are in good agreement with the theoretical predictions.

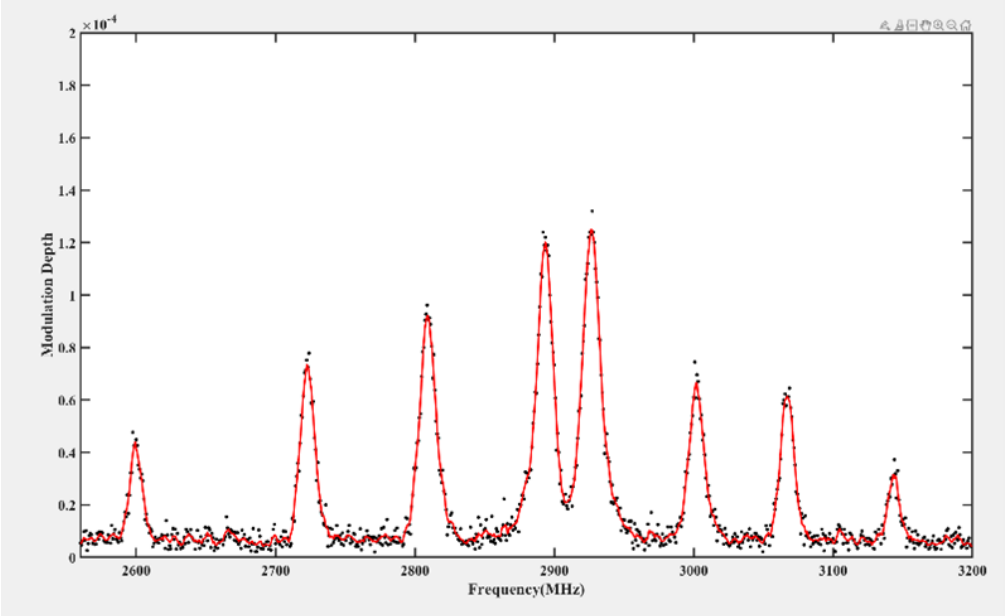

Figure 5 ODMR Spectrum Obtained from Experiments Conducted at the Center

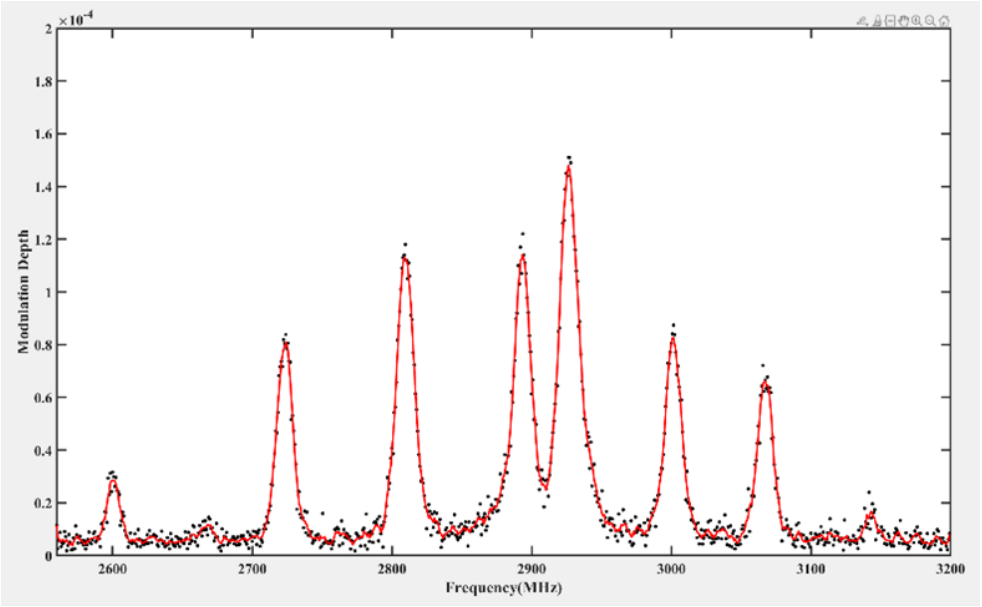

Figure 6 ODMR Spectrum Obtained from Experiments Conducted at the Edge

4. Conclusion

This paper provides a detailed derivation of the impact of magnetic field gradient on the linewidth of ODMR spectra. In modern technology, whether in medicine, physics, or agriculture, the frequency of using optically detected magnetic resonance (ODMR) techniques to obtain the magnetic field vector at a specific point is increasing. This means that improving the quality of ODMR spectra has become a problem that must be addressed in future technological development. Relying on the fundamental principles of quantum mechanics, this paper demonstrates the effect of magnetic field gradient, i.e., the uniformity of the magnetic field, on the spectral linewidth. Both theory and experiments consistently show that ODMR spectra are optimal in a uniform magnetic field.

References

[1] Ladd T D, Jelezko F, Laflamme R, et al. Quantum computers[J]. nature, 2010, 464(7285): 45-53.

[2] Valiev K A. Quantum computers and quantum computations[J]. Physics-Uspekhi, 2005, 48(1): 1.

[3] Zhou Y, Stoudenmire E M, Waintal X. What limits the simulation of quantum computers?[J]. Physical Review X, 2020, 10(4): 041038.

[4] Acosta V, Hemmer P. Nitrogen-vacancy centers: Physics and applications[J]. MRS bulletin, 2013, 38(2): 127-130.

[5] Childress L, Hanson R. Diamond NV centers for quantum computing and quantum networks[J]. MRS bulletin, 2013, 38(2): 134-138.

[6] Larsson J A, Delaney P. Electronic structure of the nitrogen-vacancy center in diamond from first-principles theory[J]. Physical Review B—Condensed Matter and Materials Physics, 2008, 77(16): 165201.

[7] Foot C J. Atomic physics[M]. Oxford university press, 2005.

[8] Zheng D. Study and manipulation of photoluminescent NV color center in diamond[D]. École normale supérieure de Cachan-ENS Cachan; East China normal university (Shanghai), 2010.

[9] Kastler A. Optical methods of atomic orientation and of magnetic resonance[J]. JOSA, 1957, 47(6): 460-465.

[10] Glaser E R, Carlos W E, Braga G C B, et al. Characterization of nitrides by electron paramagnetic resonance (EPR) and optically detected magnetic resonance (ODMR)[J]. Materials Science and Engineering: B, 2002, 93(1-3): 39-48.